# Antiviral Activity of Digoxin and Ouabain against SARS-CoV-2 Infection and Its Implication for COVID-19

**Junhyung Cho**
Korea Centers for Disease Control and Prevention https://orcid.org/0000-0002-2569-9415
**Young Jae Lee**
Korea Centers for Disease Control and Prevention
**Je-Hyoung Kim**
Korea Centers for Disease Control and Prevention
**Sang il Kim**
Catholic University
**Sung Soon Kim**
Korea Centers for Disease Control and Prevention
**Byeong-Sun Choi**
Korea Centers for Disease Control and Prevention
**Jang-Hoon Choi** ( jhchoi@nih.go.kr )
Korea Centers for Disease Control and Prevention

**Research Article**

**Keywords:** SARS-CoV-2, COVID-19, Digoxin, Ouabain, Antiviral

**Posted Date:** June 17th, 2020

**DOI:** https://doi.org/10.21203/rs.3.rs-34731/v1



**Version of Record:** A version of this preprint was published at Scientific Reports on October 1st, 2020. See the published version at https://doi.org/10.1038/s41598-020-72879-7.

# Abstract

The current coronavirus (COVID-19) pandemic is exacerbated by the absence of effective therapeutic agents. Notably, among patients with COVID-19, 10–40% of those with cardiac injury have more comorbidities such as acute heart failure and lymphocytopenia. An efficient strategy to response this issue is drug repurposing with expecting antiviral activity and therapeutic effect. Digoxin (DIG) and ouabain (OUA) are FDA drugs for heart diseases and have antiviral activity against several coronaviruses. Thus, we aimed this study to assess antiviral activity of DIG and OUA against SARS-CoV-2 infection. The half-maximal inhibitory concentration ($IC_{50}$) of DIG, and OUA were determined at a nanomolar concentration. Progeny virus titers of single dose treatment of DIG and OUA were approximately $10^3$ and $10^4$-fold lower (> 99% inhibition) than that of non-treated control or chloroquine at 48 hour post-infection (hpi). Furthermore, therapeutic treatment of DIG and OUA inhibited over 99 % of SARS-CoV-2 replication, leading to viral inhibition at post entry stage of the virus life cycle. Collectively, these results suggested that DIG and OUA could be an alternative treatment for COVID-19 with potential therapeutic effect for patients with cardiovascular disease.


# Introduction

Human coronaviruses (HCoV) are enveloped, positive-sense single-stranded RNA viruses. Six coronaviruses, namely HCoV-229E, HCoV-OC43, HCoV-HKU1, HCoV-NL63, severe acute respiratory syndrome coronavirus (SARS-HCoV) and Middle East respiratory syndrome coronavirus (MERS-HCoV) are responsible for respiratory illnesses in human. Of these, SARS-CoV and MERS-CoV infection results in severe acute respiratory disease and have caused worldwide awareness of these illnesses[1].

In December 2019, a novel coronavirus was identified in a group of patients with pneumonia in Wuhan, Hubei province, China[2]. Subsequently, the International Committee on Taxonomy of Viruses (ICTV) named this virus severe acute respiratory syndrome coronavirus 2 (SARS-CoV-2), which is the causative agent of coronavirus disease 19 (COVID-19)[3]. Owing to the substantial increase in the number of confirmed cases of COVID-19 through human-to-human transmission, a large epidemic occurred in Wuhan[4]. As SARS-CoV-2 spread to more than 216 countries, the World Health Organization (WHO) declared an ongoing pandemic on March 11 2020[5]. As of 5 June 2020, more than 6 million confirmed cases and 387,298 deaths have been reported worldwide[6].

The common symptoms of patients with COVID-19 are mild such as fever (80–98%), cough (34–76%), and shortness of breath (28–70%) and most are asymptomatic[7-10]. However, some cases have been associated with severe pneumonia, acute cardiac injury, multi-organ failure, and death[4,10-12]. Notably, among patients with COVID-19, 10–40% of those with cardiac injury have more comorbidities, including hypertension and lymphocytopenia, which result in a higher mortality rate than patients without cardiac injury (51.2% *vs.* 5.1%)[7,8,11,13,14].

No approved vaccine or specific antiviral agent is yet available for COVID-19. One of the fastest and most practical strategies to address this issue is to identify preexisting approved drugs with antiviral activity against SARS-CoV-2. Accordingly, numerous clinical trials and studies are underway to evaluate vaccines and therapeutics with the most advanced clinical trial-repurposed drugs being (hydroxy)chloroquine and remdesivir, the latter of which has received emergency use authorization by the U.S. Food and Drug Administration (FDA) on May 1, 2020[15,16]. Moreover, the WHO announced a large global clinical trial, SOLIDARITY, to assess the therapeutic effects of four repurposed drugs on March 18, 2020.

In addition to antiviral drugs based on viral protease inhibitors and nucleoside analogs, the cardiac glycoside (CG)-based drugs digoxin (DIG) and ouabain (OUA) have been shown to exhibit antiviral activity through various mechanisms against several DNA and RNA viruses, such as cytomegalovirus, herpes simplex virus, MERS-CoV, human immunodeficiency virus, respiratory syncytial virus, chikungunya virus, and the recently identified SARS-CoV-2[17-24].

Notably, these agents have been used to treat various heart diseases and were mainly identified to bind to the transmembrane protein sodium/potassium ATPase ($Na^+/K^+$-ATPase) and inhibit ion-exchange, leading to increased intracellular $Ca^{++}$ concentration and heart muscle contraction[25-27]. Therefore, in this study, we evaluated the antiviral activity of DIG and OUA by examining the viral growth kinetics and treatment conditions and compared it to that of vehicle (DMSO) or chloroquine (CHQ), in order to identify a suitable and potent antiviral agent to treat COVID-19 patients with cardiac diseases.

# Results

### Determination of half maximal inhibitory, cell cytotoxic concentration, and selective index value of DIG and OUA

To assess the antiviral activity and cell cytotoxicity of DIG and OUA against SARS-CoV-2 infection, we investigated the half-maximal inhibitory concentration ($IC_{50}$), cytotoxicity concentration 50% ($CC_{50}$), and selective index (SI) compared to those of CHQ. Vero cells were infected with BetaCoV/Korea/KCDC03/2020 at a multiplicity of infection (MOI) of 0.01 in the presence of OUA and DIG (0.0125, 0.025, 0.05, 0.1, 0.125, 0.25, 0.5, and 1 μM), and CHQ (0.125, 0.25, 0.5, 1, 2, 5, 10, and 20 μM) for 1 h and incubated with the respective drug for 24 h. The viral copy numbers in the cell culture supernatant were determined by amplifying the nucleocapsid (*N*) gene by quantitative real-time PCR (qRT-PCR) and cell viability was measured using the PrestoBlue™ Cell Viability reagent. The $IC_{50}$ values of DIG ($IC_{50}$ = 0.043 μM) and OUA ($IC_{50}$ = 0.024 μM) were determined at a nanomolar concentration and were over 10-fold lower than those of CHQ ($IC_{50}$ = 0.526 μM)(Figure 1A-C). In addition, the SI ($CC_{50}/IC_{50}$) values of DIG ($CC_{50}$ > 10 μM, SI > 232.55) and OUA ($CC_{50}$ > 10 μM, SI > 416.66) were > 5-fold than those of CHQ ($CC_{50}$ > 20 μM, SI > 38.02) (Figure 1A-C).

### Antiviral activity of DIG and OUA based on SARS-CoV-2 growth kinetics

To evaluate antiviral activity of drugs based on SARS-CoV-2 growth kinetics, cells were treated with optimal concentrations of DIG (150 nM), OUA (100 nM), and CHQ (10 μM), which inhibited over 95% of viral *N* mRNA expression at 24 hpi (Figure S1A-D).

After treating the virus-infected cells with drugs, viral *N* mRNA expression, viral copy number, and progeny virus titer were measured at 8, 24, and 48 h (the time of complete virus replication as assessed via growth kinetics)(Figure 2A-C). Viral *N* mRNA expression was almost fully suppressed (> 99%) by all drugs at 8 and 24 hpi. However, the expression of viral *N* mRNA was significantly restored in CHQ-treated cells at 48 hpi (Figure 2A). Viral copy numbers were also markedly reduced at 48 h only in the DIG- and OUA-treated cell culture supernatants (Figure 2B). Progeny virus titer in the culture medium of DIG and OUA treatment, as measured using the plaque assay, revealed a $10^3$- and $10^4$-fold reduction, respectively, and an inhibition ratio of > 99% for the drugs compared to those for the carrier (DMSO, $1.80 \times 10^6$ plaque forming units (pfu)/mL). Moreover, the virus titer was lower in the cells treated with DIG ($1.83 \times 10^3$ pfu/mL) and OUA ($1.80 \times 10^2$ pfu/mL) than with CHQ ($2.45 \times 10^6$ pfu/mL) at 48 hpi (Figure 2C, S2, and Table 1).

### Determination of the inhibition step of SARS-CoV-2 life cycle by the drug treatment

To determine which step of the virus life-cycle is inhibited by the drug treatment, DIG, OUA, and CHQ were administered at different time points of treatment, respectively, namely prophylactic (1 h prior to infection and maintenance for 24 h), entry (0 h of infection and maintenance for 2 h), and therapeutic (2 h following infection and maintenance for 24 h). All drugs demonstrated high efficacy upon prophylactic administration. The viral mRNA expression, copy number, and viral N protein expression were lower in prophylactic-treated cells than in non-treated cells by approximately 99% (Figure 3). Upon administration following entry, CHQ and OUA afforded 50% inhibition, whereas DIG treatment did not effectively inhibit virus propagation (Figure 3A-C). In comparison, OUA and DIG but not CHQ treatment significantly reduced viral replication in the therapeutic time point (Figure 3A-C).

# Discussion

SARS-CoV-2 infection causes not only multiple organ failure but also higher mortality rate in patients with underlying cardiac diseases[4,28,29]. Notably, the angiotensin-converting enzyme 2 (ACE2) receptor, which serves as a functional receptor for coronaviruses, is systemically distributed in multiple organs and is especially highly expressed in the heart and lungs[29]. Therefore, these organs may be directly or indirectly attacked by SARS-CoV-2, resulting in substantially elevated levels of proinflammatory cytokines[30-35].

The drugs, DIG and OUA, have been used for treating heart conditions in humans for over 10 decades, and thus their clinical dosage regimen, bioavailability, pharmacokinetic profile information, and safety are well known[27]. Hence, these drugs may exert multiple benefits in patients with COVID-19 in terms of antiviral and symptom management along with safety.

In this study, single dose of DIG and OUA treatment consistently showed superior antiviral activity against human isolate BetaCoV/Korea/KCDC03/2020 infection, as evident from the evaluation of viral mRNA expression, copy number (released virions in cell supernatant), and progeny virus titer until 48 hpi *in vitro*. The progeny virus titer at 48 hpi in DIG and OUA treatment groups was reduced over $10^3$-$10^4$-fold compared to either non-treated vehicle (DMSO) or CHQ groups, indicating that DIG and OUA have effective antiviral activity with stability until 48 hpi (this time point represents the peak viral titer on growth kinetics in Vero cells, corresponding to maximal SARS-CoV-2 replication)[36]. This result suggested that the antiviral activity of DIG and OUA is more effective than that of CHQ, which was recently reported as an effective treatment against SARS-CoV-2 by drug repositioning[37].

Notably, DIG and OUA significantly inhibited viral mRNA expression, copy number and viral protein expression when administered at the post-entry stage, although DIG did not show effective antiviral activity at the host entry stage of the virus cycle. Clinically, this result is very important for therapeutics, as a large numbers of patients are asymptomatic at the initial stage of SARS-CoV-2 infection[38,39]. Moreover, this indicated that the inhibition mechanism of SARS-CoV-2 by DIG may be similar to that of RSV, wherein inhibition occurs at the step of viral RNA synthesis[18]. However, OUA may be different mechanism from DIG, which OUA treatment at entry stage inhibited approximately 50% of viral mRNA expression and protein expression. Thus, further study will be necessary to investigate the antiviral mechanism of DIG and OUA against SARS-CoV-2 infection.

Taken together, we demonstrated that effective antiviral activity of DIG and OUA against human isolate SARS-CoV-2 infection on viral growth kinetics and application stage of the virus life cycle. It is suggested that these agents could serve as therapeutic options for patients with COVID-19 and comorbid cardiac diseases. Interestingly, previous studies on heart diseases have identified that proinflammatory cytokine level, such as of TNF-α, was up-regulated and treatment with anti-TNF antibody improved survival in human cardiac disease animal model[40,41]. This suggested that DIG and OUA might have an additional therapeutic role against COVID-19 with hypercytokinemia, as it was a recently reported that digitoxin, one of CG, suppresses proinflammatory cytokines including TNF-α in influenza A virus-infected cotton rat lung[42]. Further study will be necessary to investigate the antiviral activity of DIG and OUA against SARS-CoV-2 infection in human cardiac disease animal model with management of cardiac injury and hyper immune response, as a first step of these drugs to clinical trials.

# Materials And Methods

### Virus, cells, compounds, and infection

BetaCoV/Korea/KCDC03/2020 (GISSAID accession ID: EPI_ISL_407193) was obtained from the National Culture Collection for Pathogens of Korea Center for Diseases Control and prevention (KCDC)[43]. Vero cells were purchased from the American Type Culture Collection (ATCC® CCL-81™, Manassas, VA, USA) and cultured in Dulbecco's minimal essential medium

(DMEM; Gibco, Grand Island, NY, USA) supplemented with 2 (infection media) or 10% (growth media) v/v heat inactivated fetal bovine serum (FBS; Gibco) and 1% v/v penicillin/streptomycin (p/s; Gibco) in a humidified incubator of 5% $CO_2$ atmosphere at 37 °C. OUA, CHQ, and DIG were purchased from Sigma-Aldrich (St. Louis, MO, USA). DIG tablets (inno. N, Seoul, Korea) were provided by Dr. Sang il Kim. OUA and DIG tablets were dissolved in $H_2O$ and CHQ and DIG were dissolved in DMSO. Confluent Vero cells were infected at an MOI of 0.01 of BetaCoV/Korea/KCDC03/2020 in DMEM containing 2% FBS (infection media) and 1% p/s for 1 h. Following incubation, cells were washed twice with phosphate buffered saline (PBS; Gibco) and incubated in the infection media. All experiments were performed in biosafety level 3 facilities according to Korea Center for Disease Control (KCDC) procedures.

### Cloning and linearity determination of the RNA reference

The PCR products with SARS-CoV-2 N primers were cloned into pGEM-T Easy Vector (Promega, Madison, WI, USA) and in vitro transcribed using the RiboMAXTM Large Scale RNA Production System-T7 (Promega). The linearity of the RNA reference template was evaluated with a 10-fold serial dilution of in vitro transcribed N RNA of SARS-CoV-2 ($10^4$–$10^{10}$ copies). The copy number of RNA was calculated using: [X g/μL RNA/(transcript length in nucleotides – 340)] × 6.022 × $10^{23}$ = Y molecules/μL[44]. The linear range was determined using a standard curve generated with diluted reference RNAs and the best-fit line to the raw data was established by linear regression analysis with 95% confidence intervals using GraphPad Prism (version 5.01; La Jolla, CA, USA).

### Quantitative real-time PCR (qRT-PCR)

For the quantification of viral copy number, total RNA was isolated from cell supernatants using the QIAamp viral RNA mini kit (QIAGEN, Hilden, Germany) and cDNA was synthesized from 1 μg of total RNA using SuperScript IV (Invitrogen, Waltham, MA, USA) according to the manufacturer's protocol. qRT-PCR was performed using Power SYBR Green PCR master mix (Applied Biosystems, Foster City, CA, USA) and an Applied Biosystems™ QuantStudio3™ (Applied Biosystems) following the manufacturer's protocol.

For the measurement of viral mRNA, total RNA was isolated from the cell using TRIzol™ (Ambion, Leicestershire, UK) reagent. Subsequently, cDNA was synthesized from 1 μg of total RNA using a SuperScript IV (Invitrogen). qRT-PCR was performed using Power SYBR Green PCR master mix (Applied Biosystems) and Applied Biosystems™ QuantStudio3™ (Applied Biosystems) as follows: denaturation at 95 ℃ for 5 min, followed by 40 cycles of 95 ℃ for 30 s and 60 ℃ for 30 s. The sequences of the *GAPDH* primers used were: 5¢-GAA CGG GAA GCT TGT CAT CAA TGG-3¢ and 5¢-TGT GGT CAT GAG TCC TTC CAC GAT-3¢. The sequences of the *N* primers used were: 5¢-GGG AGC CTT GAA TAC ACC AAA A-3¢ and 5¢-TGT AGC ACG ATT GCA GCA TTG-3¢[45]

### Western blotting

Vero cells were lysed in Pierce RIPA buffer (Thermo Scientific, Waltham, MA, USA) and 20 μg of protein was separated using Bolt™ 4-12% Bis-Tris Plus (Invitrogen). Proteins were detected by probing the membranes with 1:1,000 anti-SARS-CoV-2 nucleocapsid (Sino Bio., Beijing, China) and 1:2,000 anti-β-actin (Cell Signaling Technologies, Danvers, MA, USA) antibodies. Protein transfer was performed using iBlot 2 (Invitrogen) and iBlot 2 PVDF Regular Stacks (Invitrogen). Membranes were incubated with goat anti-rabbit antibody (Cell Signaling) conjugated with horseradish peroxidase for 1 h. Then, membranes were washed five times with tris-buffered saline with 5% Tween 20. Thereafter, the blots were detected using Super Signal™ (Thermo Scientific).

### Plaque assay

Monolayers of Vero cells were prepared in 12-well plates. The cells were infected with 10-fold serial dilutions of the supernatant of the indicated treatments and incubated at 37 °C for 1 h. The medium was removed and cells were washed

with PBS. Each well was overlaid with MEM/agarose (Gibco) and maintained at room temperature until the overlay turned solid. The plates were incubated at 37 °C for 3 days. Then, the cells were fixed with 2% paraformaldehyde (Thermo Scientific) and stained with 1% crystal violet (Sigma-Aldrich) overnight.

### $IC_{50}$ and $CC_{50}$ measurements

Confluent Vero cells in 12-well plates were pre-treated with eight concentrations of OUA and DIG (0.0125, 0.025, 0.05, 0.1, 0.125, 0.25, 0.5, and 1 μM), and CHQ (0.125, 0.25, 0.5, 1, 2, 5, 10, and 20 μM) for 1 h in DMEM containing 2% FBS and 1% p/s. After incubation, an MOI of 0.01 of BetaCoV/Korea/KCDC03/2020 was added to cells for 1 h and cells were washed twice with PBS and a new medium was added with the indicated concentrations of the drugs for 24 h. Subsequently, cell viability was measured using the PrestoBlue™ Cell Viability reagent (Invitrogen, Waltham, MA, USA) and viral RNA was isolated from cell supernatants and cDNA was synthesized. qRT-PCR was performed using Power SYBR Green PCR master mix (Applied Biosystems) and Applied Biosystems™ QuantStudio3™. The copy number was calculated based on the reference RNA template and the $IC_{50}$ value was calculated using GraphPad Prism.

### Drug treatment

Vero cells were pre-treated with DIG (150 nM), OUA (100 nM), or CHQ (10 μM) for 1 h, and then the virus was applied for 1 h to allow infection. The drug-virus mixture was removed and the cells were washed twice with PBS. Subsequently, the cells were incubated in the presence of fresh medium containing the optimal concentrations of the drugs and the cells and supernatant were collected at 8, 24, and 48 hpi for quantification of viral mRNA, copy number, and progeny virus titer.

For the prophylactic condition, Vero cells were pre-treated with the drugs in infection medium for 1 h and the virus was applied for 1 h to allow infection. Subsequently, the cells were washed twice with PBS and incubated for 24 h in the presence of the drugs in fresh infection medium.

For the entry condition, the cells were treated with the drugs for the infection period (1 h), followed by removal of the drug-virus mixture and washing of the cells. Subsequently, the cells were incubated in infection medium without the drugs for 24 h.

For therapeutic condition, following viral infection without the drugs for 1 h, the virus was discarded and the cells were washed. Then, the drugs in fresh infection medium were applied to the cells for 24 h. Following incubation, the cells were used for virus mRNA quantification and investigation of virus protein expression and the supernatant was used for counting virus yield.

### Statistical analysis

The statistical significance of DMSO control and drug treatments were assessed by one-way ANOVA with Dunnett's multiple comparison test. The statistical comparison of the viral copy number, mRNA expression, and progeny virus titer was done using two-way ANOVA with Bonferroni post-tests. Data plotting and statistical analysis were performed using GraphPad Prism. A $P$ value < 0.05 was considered statistically significant.

## Declarations


### Acknowledgements

This research was supported by the Korea National Institute of Health fund (2019-NI-070-01).


### Author Contributions

J.C, J.H.C, and B.S.C. designed the experiments. J.C, and J.H.C wrote the manuscript. J.C, Y.J.L, and J.H.K conducted many of experiments (J.C performed virus infection, qPCR, and western blotting; Y.J.L conducted plaque assay; J.H.K performed qRT-PCR and analysis data of virus copy number). S.I.K provided digoxin tablet and S.I.K and S.S.K advised clinical and pharmacological aspect of the drugs. J.H.C. and B.S.C. supervised the experiments and revised the manuscript.

**Additional Information**

**Competing financial interests:** the authors declare no competing financial interests.

# References


1 Su, S. *et al.* Epidemiology, Genetic Recombination, and Pathogenesis of Coronaviruses. *Trends Microbiol.* **24**, 490-502, doi:10.1016/j.tim.2016.03.003 (2016).

2 Zhu, N. *et al.* A Novel Coronavirus from Patients with Pneumonia in China, 2019. *N. Engl. J. Med.* **382**, 727-733, doi:10.1056/NEJMoa2001017 (2020).

3 ICTV. Naming the 2019 coronavirus. *http://talk.ictvonline.org/* (2020).

4 Hui, D. S. *et al.* The continuing 2019-nCoV epidemic threat of novel coronaviruses to global health - The latest 2019 novel coronavirus outbreak in Wuhan, China. *Int. J. Infect. Dis.* **91**, 264-266, doi:10.1016/j.ijid.2020.01.009 (2020).

5 World Health Organization (WHO). WHO Director-General's opening remarks at the media briefing on COVID-19. https://www.who.int/dg/speeches/detail/who-director-general-s-opening-remarks-at-the-media-briefing-on-covid-19—11-march-2020 (2020).

6 World Health Organization (WHO). Coronavirus disease (COVID-19) outbreak situation. https://www.who.int/emergencies/diseases/novel-coronavirus-2019?gclid=Cj0KCQjwoPL2BRDxARIsAEMm9y_2o8RtKOqhgZuzXq1021Xw8yuLIV7iopd9crZU1zVmv73jUkTemN8aArjQEALw_wcB (2020).

7 Shi, S. *et al.* Association of cardiac injury with mortality in hospitalized patients with COVID-19 in Wuhan, China. *JAMA Cardiol.* E1-E8 (2020).

8 Huang, C. *et al.* Clinical features of patients infected with 2019 novel coronavirus in Wuhan, China. *Lancet* **395**, 497-506 (2020).

9 Wang, D. *et al.* Clinical characteristics of 138 hospitalized patients with 2019 novel coronavirus–infected pneumonia in Wuhan, China. *JAMA* **323**, 1061-1069 (2020).

10 Centers for Disease Control and Prevention (CDC), U. Symptoms of Coronavirus. https://www.cdc.gov/coronavirus/2019-ncov/symptoms-testing/symptoms.html (2020a).

11 Chen, N. *et al.* Epidemiological and clinical characteristics of 99 cases of 2019 novel coronavirus pneumonia in Wuhan, China: a descriptive study. *Lancet* **395**, 507-513, doi:10.1016/S0140-6736(20)30211-7 (2020).

12 Day, M. Covid-19: four fifths of cases are asymptomatic, China figures indicate. *BMJ* **369**, m1375, doi:10.1136/bmj.m1375 (2020).

13 Madjid, M., Safavi-Naeini, P., Solomon, S. D. & Vardeny, O. Potential effects of coronaviruses on the cardiovascular system: a review. *JAMA Cardiol.* E1-E10 (2020).

14 Yang, X. *et al.* Clinical course and outcomes of critically ill patients with SARS-CoV-2 pneumonia in Wuhan, China: a single-centered, retrospective, observational study. *The Lancet Respiratory Medicine,* **8**, 475-481 (2020).

15 Dhama, K. *et al.* COVID-19, an emerging coronavirus infection: advances and prospects in designing and developing vaccines, immunotherapeutics, and therapeutics. *Hum. Vaccin. Immunother.*, 1-7, doi:10.1080/21645515.2020.1735227 (2020).

16 Sanders, J. M., Monogue, M. L., Jodlowski, T. Z. & Cutrell, J. B. Pharmacologic treatments for coronavirus disease 2019 (COVID-19): a review. *JAMA* **323**, 1824-1836 (2020).

17 Amarelle, L. & Lecuona, E. The Antiviral Effects of Na,K-ATPase Inhibition: A Minireview. *Int. J. Mol. Sci.* **19,** doi:10.3390/ijms19082154 (2018).

18 Norris, M. J. *et al.* Targeting intracellular ion homeostasis for the control of respiratory syncytial virus. *Am. J. Respir. Cell Mol. Biol.* **59**, 733-744 (2018).

19 Dodson, A. W., Taylor, T. J., Knipe, D. M. & Coen, D. M. Inhibitors of the sodium potassium ATPase that impair herpes simplex virus replication identified via a chemical screening approach. *Virology* **366**, 340-348 (2007).

20 Ganesan, V. K., Duan, B. & Reid, S. P. Chikungunya virus: pathophysiology, mechanism, and modeling. *Viruses* **9**, 368 (2017).

21 Kapoor, A. *et al.* Human cytomegalovirus inhibition by cardiac glycosides: evidence for involvement of the HERG gene. *Antimicrob. Agents Chemother.* **56**, 4891-4899 (2012).

22 Laird, G. M., Eisele, E. E., Rabi, S. A., Nikolaeva, D. & Siliciano, R. F. A novel cell-based high-throughput screen for inhibitors of HIV-1 gene expression and budding identifies the cardiac glycosides. *J. Antimicrob. Chemother.* **69**, 988-994 (2014).

23 Yang, C.-W., Chang, H.-Y., Lee, Y.-Z., Hsu, H.-Y. & Lee, S.-J. The cardenolide ouabain suppresses coronaviral replication via augmenting a Na+/K+-ATPase-dependent PI3K_PDK1 axis signaling. *Toxicol. Appl. Pharmacol.* **356**, 90-97 (2018).

24 Jeon, S. *et al.* Identification of antiviral drug candidates against SARS-CoV-2 from FDA-approved drugs. *Antimicrob. Agents Chemother.* doi: 10.1128/AAC.00819-20 (2020).

25 Dvela, M., Rosen, H., Feldmann, T., Nesher, M. & Lichtstein, D. Diverse biological responses to different cardiotonic steroids. *Pathophysiology* **14**, 159-166 (2007).

26 Fürstenwerth, H. Ouabain-the insulin of the heart. *Int. J. Clin. Pract.* **64**, 1591 (2010).

27 Rahimtoola, S. H. & Tak, T. The use of digitalis in heart failure. *Curr. Probl. Cardiol.* **21**, 781-853 (1996).

28 Kang, Y. J. Mortality Rate of Infection With COVID-19 in Korea From the Perspective of Underlying Disease. *Disaster Med. Public Health Prep.*, 1-3, doi:10.1017/dmp.2020.60 (2020).

29 Zou, X. *et al.* Single-cell RNA-seq data analysis on the receptor ACE2 expression reveals the potential risk of different human organs vulnerable to 2019-nCoV infection. *Front. Med.* **14**, 185-192 (2020).

30 Akhmerov, A. & Marbán, E. COVID-19 and the heart. *Circ. Res.* **126**, 1443-1455 (2020).

31 Cao, X. COVID-19: immunopathology and its implications for therapy. *Nat. Rev. Immunol.* **20**, 269-270 (2020).

32 Ong, E. Z. *et al.* A Dynamic Immune Response Shapes COVID-19 Progression. *Cell Host Microbe,* **27**, 1-4, doi: 10.1016/j.chom.2020.03.021. (2020).

33 Qin, C. *et al.* Dysregulation of immune response in patients with COVID-19 in Wuhan, China. *Clin. Infect. Dis.* doi: 10.1093/cid/ciaa248. (2020).

34 Shi, Y. *et al.* Immunopathological characteristics of coronavirus disease 2019 cases in Guangzhou, China. *MedRxiv,* doi: 10.1101/2020.03.12.20034736 (2020).

35 Xu, Z. *et al.* Pathological findings of COVID-19 associated with acute respiratory distress syndrome. *Lancet Resp. Med.* **8**, 420-422 (2020).

36 Harcourt, J. *et al.* Isolation and characterization of SARS-CoV-2 from the first US COVID-19 patient. *BioRxiv,* doi: 10.1101/2020.03.02.972935 (2020).

37 Wang, M. *et al.* Remdesivir and chloroquine effectively inhibit the recently emerged novel coronavirus (2019-nCoV) in vitro. *Cell Res.* **30**, 269-271 (2020).

38 Backer, J. A., Klinkenberg, D. & Wallinga, J. Incubation period of 2019 novel coronavirus (2019-nCoV) infections among travellers from Wuhan, China, 20–28 January 2020. *Eurosurveillance* **25**, 2000062 (2020).

39 Zheng, Y. Y., Ma, Y. T., Zhang, J. Y. & Xie, X. COVID-19 and the cardiovascular system. *Nat. Rev. Cardiol.* **17**, 259-260, doi:10.1038/s41569-020-0360-5 (2020).

40 Hasenfuss, G. Animal models of human cardiovascular disease, heart failure and hypertrophy. *Cardiovasc. Res.* **39**, 60-76 (1998).

41 Matsumori, A. & Sasayama, S. Immunomodulating agents for the management of heart failure with myocarditis and cardiomyopathy—lessons from animal experiments. *Eur. Heart J.* **16**, 140-145 (1995).

42 Pollard, H. B., Pollard, B. S. & Pollard, J. R. Classical drug digitoxin inhibits influenza cytokine storm, with implications for COVID-19 therapy. *bioRxiv* (2020).

43 Kim, J.-M. *et al.* Identification of Coronavirus Isolated from a Patient in Korea with COVID-19. *Osong Public Health and Research Perspectives* **11**, 3 (2020).

44 Kim, J.-H. *et al.* Clinical diagnosis of early dengue infection by novel one-step multiplex real-time RT-PCR targeting NS1 gene. *J. Clin. Virol.* **65**, 11-19 (2015).

45 Centers for Disease Control and Prevention (CDC). Research use only 2019-novel coronavirus (2019-nCoV) real-time RT-PCR primer and probe information. https://www.cdc.gov/coronavirus/2019-ncov/lab/rt-pcr-panel-primer-probes.html. (2020b)

# Tables

Table 1. Progeny virus titer in cell supernatant

| Time (hpi) | Drug | Pfu/mL |
|---|---|---|
| 8 | DMSO | $3.07_{\times 10^{3}}$ |
| | Digoxin | $1.67_{\times 10^{1}}$ |
| | Ouabain | $1.67_{\times 10^{1}}$ |
| | Chloroquine | $1.60_{\times 10^{2}}$ |
| 24 | DMSO | $3.90_{\times 10^{6}}$ |
| | Digoxin | $1.43_{\times 10^{3}}$ |
| | Ouabain | $6.53_{\times 10^{2}}$ |
| | Chloroquine | $1.37_{\times 10^{4}}$ |
| 48 | DMSO | $1.80_{\times 10^{6}}$ |
| | Digoxin | $1.83_{\times 10^{3}}$ |
| | Ouabain | $1.80_{\times 10^{2}}$ |
| | Chloroquine | $2.45_{\times 10^{6}}$ |

# Figures

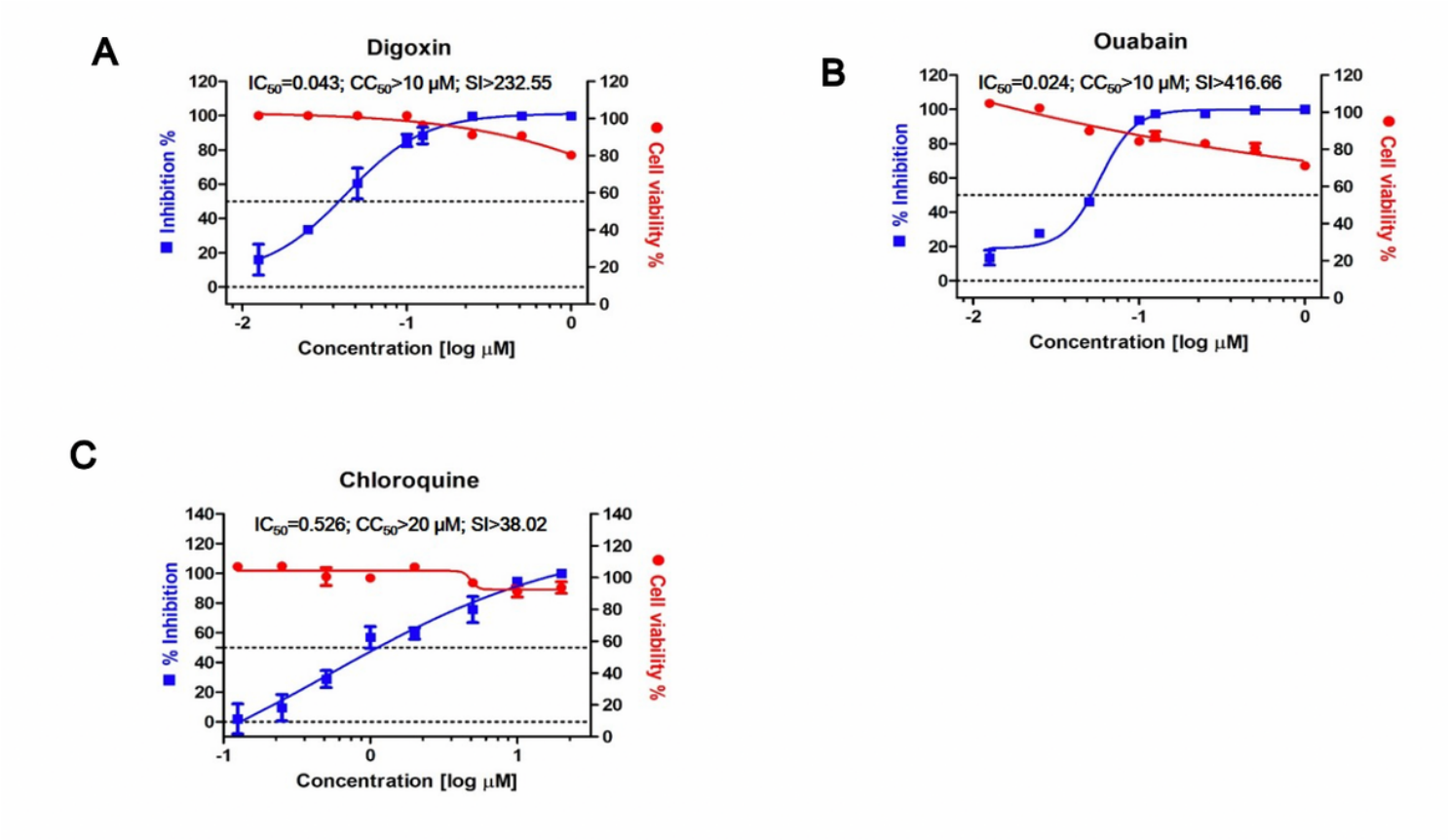


## Figure 1

Half maximal inhibitory concentration (IC50), cytotoxic concentration (CC50) and selective index (SI) of digoxin, ouabain, and chloroquine against SARS- CoV-2 infection. IC50 (left axis, blue square) and CC50 (right axis, red circle) and SI of (A) digoxin (DIG), (B) ouabain (OUA), and (C) chloroquine (CHQ). Vero cells were infected with BetaCoV/Korea/KCDC03/2020 at an MOI of 0.01 in the presence of the indicated drug concentration and were incubated for 24 h. IC50 and CC50 were determined from dose response curves based on treatment with eight concentrations. IC50 were determined by viral copy number based on standard curve, and CC50 was investigated by cell viability assay. Viral copy number of DMSO was set to 100 %, and the rests were represented as means ± SD (n=3).

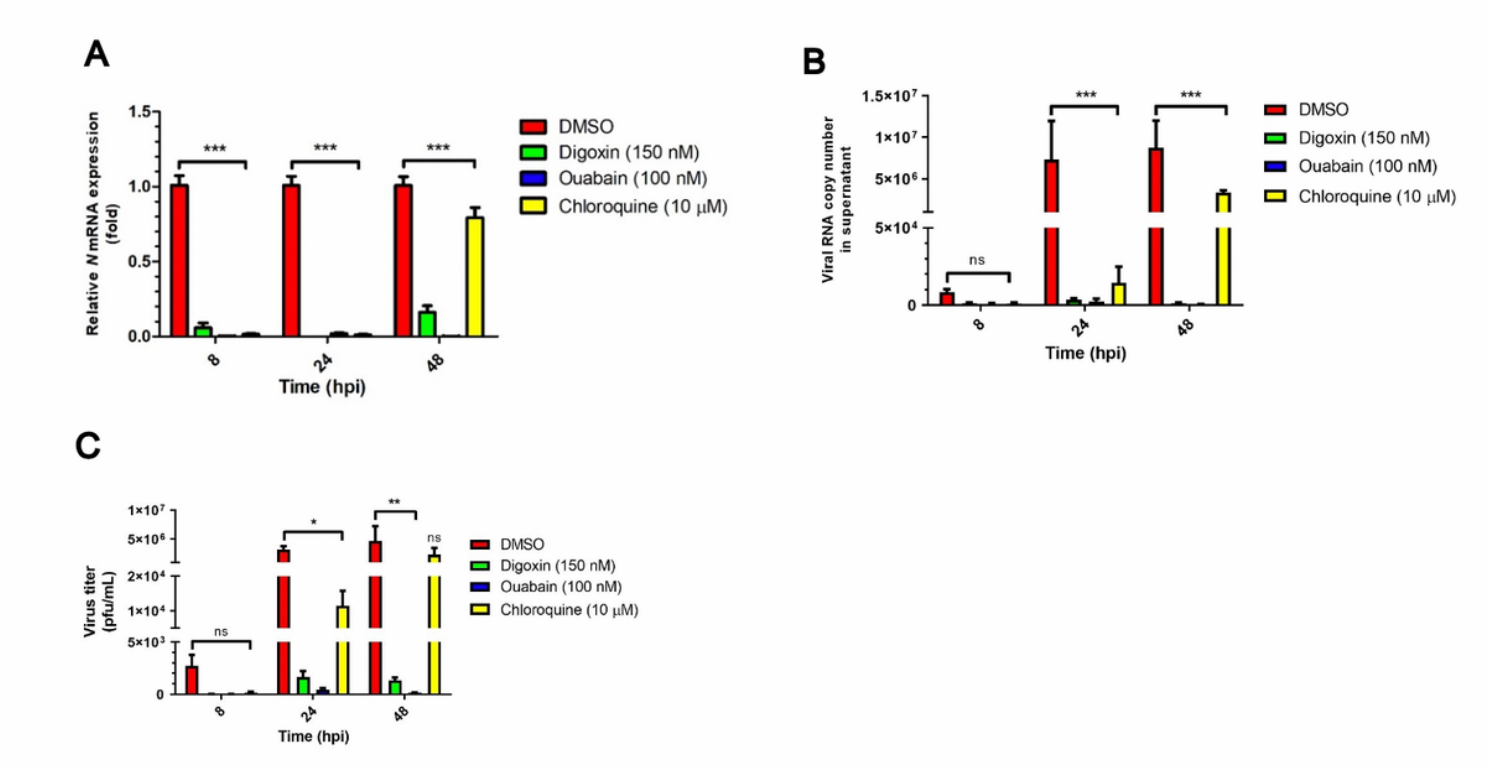


## Figure 2

Antiviral activity of digoxin, ouabain and chloroquine on SARS-CoV-2 growth kinetics. Vero cells were infected with BetaCoV/Korea/KCDC03/2020 at an MOI of 0.01 and were incubated in the presence of digoxin (150 nM), ouabain (100 nM), and chloroquine (10 μM) for 8, 24, and 48 hpi. At each time point, (A) viral mRNA expression, (B) viral copy number, and (C) progeny titer were assessed using qRT-PCR and plaque assay. Viral mRNA expression was normalized to GAPDH expression. DMSO was set to 1. Viral copy number was calculated on standard curve. Values are presented as mean ± SD (n=3). Statistically significantly differences between DMSO and drug treatment are represented as *P < 0.05, **P < 0.01, and ***P < 0.001 determined using the two-way ANOVA with Bonferroni post-tests (each column compared to control). Abbreviation: ns, not significant.

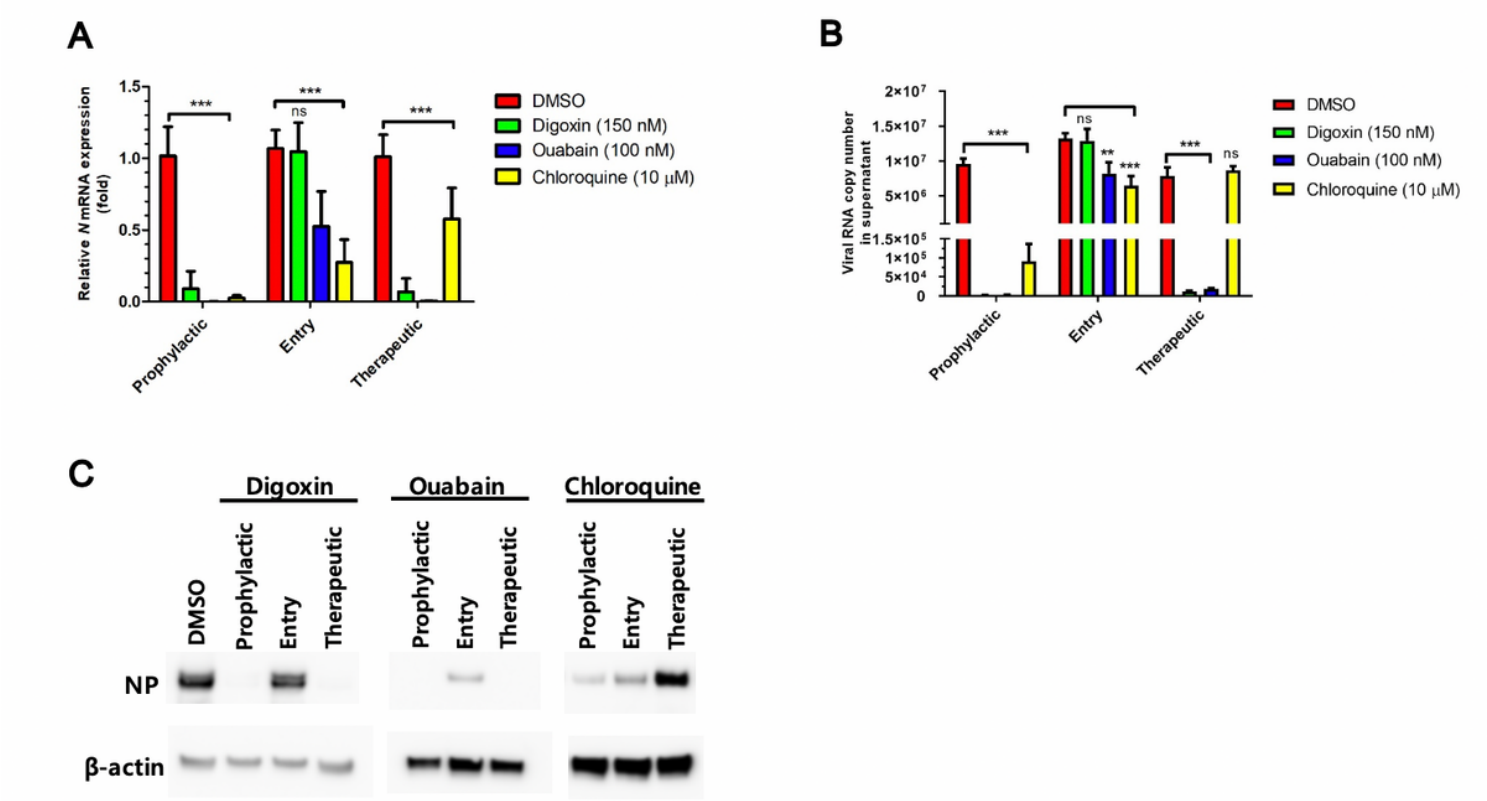


**Figure 3**

Determination of inhibition step of each drug in SARS-CoV-2 life cycle. Vero cells were infected with BetaCoV/Korea/KCDC03/2020 at an MOI of 0.01 and treated with digoxin (150 nM), ouabain (100 nM), and chloroquine (10 μM) in prophylactic, entry and therapeutic conditions. Then, the cells were incubated under the presence of the indicated drugs for 24 h. (A) Viral mRNA expression, (B) viral copy number, and (C) viral N protein expression were investigated using qRT-PCR and western blotting (also see Figure S3). Viral mRNA expression was normalized to GAPDH levels. Values are presented as mean ± SD (n=3). Anti-β-actin blots were used as loading controls. Statistically significantly differences between DMSO and drug treatment are represented as **P < 0.01, and ***P < 0.001 determined using the two-way ANOVA with Bonferroni post-tests. Abbreviation: ns, not significant.

## Supplementary Files

This is a list of supplementary files associated with this preprint. Click to download.

- SupplementaryInformation.docx